

D17

N81-14155

EFFECTS OF THE SHUTTLE ORBITER FUSELAGE AND ELEVON
ON THE MOLECULAR DISTRIBUTION OF WATER VAPOR FROM THE
FLASH EVAPORATOR SYSTEM

by

Robert G. Richmond and Robert M. Kelso

ABSTRACT

A concern has arisen regarding the emissive distribution of water molecules from the Shuttle Orbiter Flash Evaporator System (FES). The role of the Orbiter fuselage and elevon in affecting molecular scattering distributions was unclear. An experiment was conducted at NASA-Johnson Space Center to evaluate the effect of these components. Molecular distributions of the water-vapor effluents from the FES were measured. These data are compared with analytically predicted values and the resulting implications are discussed.

INTRODUCTION

As spacecraft, payloads, and instrumentation have become more complex and mission durations increased, contamination of spaceborne optical systems has been shown to present significant problems (Ref. 1). With the emergence of the Space Shuttle program, more stringent cleanliness requirements in controlling contamination levels have been generated because: (1) the Shuttle is reusable and (2) payload experiments, in general, are expected to be more contamination-sensitive and utilize larger optical systems than previous spaceflights.

Recent investigations (Ref. 2) have identified several major Shuttle Orbiter on-orbit sources of contamination: (1) outgassing, (2) offgassing, (3) Shuttle Orbiter cabin atmosphere leakage, (4) supplemental flash-evaporator vents, (5) Vernier Control System (VCS) 25-lb. vernier engines, and (6) return flux (Figure 1). These sources, either steady state or transient in nature, represent the largest contributors to contamination levels on the Shuttle. Substances from these sources contribute to the on-orbit induced molecular and particulate environment in which scientific payloads will be operated. Exposure of payload experiments to this environment could result in the degradation of performance, e.g., increases in background brightness from scattering or emission of energy, or the condensation of reflected molecules on sensitive optical components and thermal-control coatings.

Experiments were conducted at the National Aeronautics and Space Administration, Johnson Space Center (NASA-JSC) to measure the distribution of water expelled through a specially-designed sonic nozzle into a thermal-vacuum environment. The nozzle was connected to an engineering model of the flight version of the flash evaporator system and the experiment was conducted in Chamber A of the Space Environment Simulation Laboratory. Water vapor was released into the chamber at various flow rates through the sonic nozzle and

the molecular fluxes of the resultant water-vapor plume were measured.

The primary objective of this series of experiments was to determine the directional characteristics of the nozzle as a function of elevon position and elevon/fuselage anticipated surface temperature extremes. These data are required to insure that excess fuel-cell water ejected overboard travels away from the Orbiter and does not reflect from spacecraft surfaces to produce an environment which could contaminate the payload experiments.

TECHNICAL BACKGROUND

The Flash Evaporator System (FES), one of four heat-rejection mechanisms integrated into the Shuttle Orbiter Active Thermal Control System (ATCS), is activated during on-orbit operation to provide two primary functions. The first function provides for ejection of excess fuel-cell water. The Shuttle Orbiter fuel-cell can generate over 650 kg/day of excess water during normal on-orbit operations. This excess fuel-cell water is ejected overboard the Orbiter by the flash evaporator through two non-propulsive, sonic nozzles at a variable frequency between 0-4 Hz (dependent on the Orbiter heat load) with a pulse width of 100ms. The second function of the flash evaporator is to provide supplemental heat rejection capability on an as-required basis when the Orbiter heat load exceeds the capability of the Shuttle radiator system. While the FES is comprised of two evaporator duct assemblies, the main evaporator, only the topping evaporator is used during payload operations because of molecular contamination considerations (Ref. 3).

Although the Flash Evaporator System assists in the reduction of the total weight of the vehicle as a result of evaporant dumping of fuel-cell water into space, subsequently reducing the size requirement of radiation panels, a major concern of the process is the increase in the contamination potential to the spacecraft and its payload experiments. Reflection of water from Shuttle wing surfaces during the evaporator operation could conceivably increase the particulate and molecular density of the induced environment of the Shuttle. Thus, it is necessary to determine the molecular flux and line-of-sight directions of the water molecules ejected by the flash evaporator.

THEORETICAL CONSIDERATIONS

A source-flow technique for modeling the spacecraft contamination in an on-orbit environment was developed for the NASA-Johnson Space Center (Ref. 4). This technique represented a reasonable approximation of the plume flow-fields and assisted in the final selection of location of plume sensors for the experiments.

The Shuttle Orbiter FES was considered as a point source in the model because at large distances from the evaporator nozzle the gas diverges radially as though it originated from a point source. The technique is primarily dependent on geometrical relationships between the angle (θ) as measured from the plume centerline of the nozzle and the distance (r) as measured from the source.

Predicted values for the molecular flux from the sonic nozzle were

determined by the relationship:

$$\phi_1 = \frac{1.93 \cos^6 (0.608 \theta)}{r^2} \text{ g/cm}^2\text{.sec} \quad \text{eq. (1)}$$

for $0^\circ \leq \theta \leq 148^\circ$

$$\text{and } \phi_2 = 0 \quad \text{g/cm}^2\text{.sec} \quad \text{eq. (2)}$$

for $148^\circ \leq \theta \leq 180^\circ$ (θ in radians)

Total flow rates for this function are 13.3 kg/hr (nominal average) and 31.7 kg/hr (maximum instantaneous). This function is shown graphically for normalized mass-flux in Figure 2.

Data from curves generated by equation (1), for variable evaporator flow rates, were used to predict the mass-flux rates for various locations in the plume flow field. These predictions were in turn used to determine where in Chamber A the plume measurement sensors should be placed.

EXPERIMENT CONFIGURATION

The general configuration for this series of experiments is shown photographically in Figure 3 and schematically in Figure 4. The basic configuration consists of four major elements: (1) the sonic nozzle, (2) the fuselage simulator, (3) the elevon simulator, and (4) the sensor and their location.

The sonic nozzle, some pertinent characteristics of which were discussed in Section III, was mounted 2.1 meters (7 feet) above the chamber floor and positioned to operate in a horizontal plane. The nozzle was installed flush with the front face of a flat panel, 1.2m by 2.1m (4' x 7') which served as a simulator of the side fuselage of the Shuttle Orbiter. The fuselage simulator was equipped with heating elements to provide temperature control of the panel between -100°C and $+40^\circ\text{C}$ during test conditions.

A rotatable panel, representing a simulation of the wing elevon of the Shuttle Orbiter, was mounted normal to the fuselage simulator. The elevon simulator angle was varied with a motor drive assembly, thereby permitting changes in the plume profile due to perturbations attributable to the elevon to be assessed. All elevon angles were measured relative to the horizontal component of the nozzle centerline. The elevon simulator was also equipped with heaters to control temperatures between -100°C and $+40^\circ\text{C}$. The nozzle, fuselage simulator and elevon simulator are shown in Figure 5.

Cryogenically-cooled quartz crystal microbalances were chosen for primary measurement of the molecular plume profile. The quartz crystal microbalance (QCM) has been a vital instrument in molecular flux measurements. The QCM has been used for several years in this laboratory to measure quantities of condensing contamination in a thermal-vacuum environment.

The QCM consists of a sensing crystal, reference crystal and associated electronics. With contamination condensing on the sensing crystal, a frequency difference, or beat frequency, is created. This beat frequency is proportional

to mass loading on the sensing crystal. Molecular flux (mass-flux) values can be established from the QCM sensitivity of 3.5×10^{-9} g/cm².H₂. Liquid nitrogen cooling adapters, Figure 6, were used in association with the QCM sensor to permit the QCM crystals to operate near cryogenic temperatures. The sensor electronics were thermally isolated. Detailed operation of the QCM has been previously reported (Ref. 5,6) and will not be discussed here. Secondary (backup) measurements were provided by ionization gages, mass spectrometers and capacitance manometers.

General sensor location is shown in Figures 4 and 6. Figure 7 gives a closer view of the instrument. Five cryogenically-cooled QCM's were installed along the chamber wall at a distance of 10 meters from the nozzle. These five sensors, expected to measure molecular flux intensities in the range 10^{-6} to 10^{-8} g/cm².sec¹, were placed at angular locations of 0°, 20°, 30°, 40°, and 60° relative to the centerline of the flash evaporator nozzle. Only the primary QCM measurements will be reported here.

All of the molecular plume sensors were installed in the horizontal plane of the flash evaporator nozzle 2.1 meters above the chamber floor. This decision was based on math modeling predictions that the flow field was symmetrical around the plume centerline.

During those test points where the QCM's were not used to acquire data, specially constructed aluminized mylar curtains were lowered in front of the QCM's located at 0°, 20°, 30°, and 40° relative to the centerline of the nozzle. Shown photographically in Figure 6, the curtains prevented line-of-sight transmission of water vapor from the evaporator to the cryogenically-cooled crystals of the QCM's during non-plume testing activities. At a chamber pressure of 10^{-6} torr the condensation coefficient for water at temperatures below -140°C is approximately unity. This means that the impingement of water vapor molecules on surfaces of temperatures of lower value (near LN₂ temperatures), viz., the QCM crystal, will result in adherence of essentially all of the molecules. Thus, the mylar curtain prevented the QCM from becoming saturated by water vapor when they were not acquiring mass flux rates high enough to cause saturation of the instrument.

EXPERIMENTAL RESULTS AND DISCUSSION

A typical mass-flux distribution is shown in Figure 8. The data represent mass flux, g/cm².sec, as a function of angle relative to the nozzle centerline. These data are for the case where the elevon/fuselage assembly is cold (-100°C), the elevon is positioned at the "nominal" 0° location, and a flow rate of about 16.5 kg/hr through the nozzle. The measured values compare quite well with those predicted by theory.

The effect of the elevon position on mass-flux distribution is shown in Figure 9. These data, representing the cold (-100°C) elevon/fuselage, again agree quite well with predicted values with one exception--when the elevon is positioned in the "stowed" configuration. Considerably higher values of mass-flux were measured at the 30° and 40° angles than were anticipated, possibly indicating some scatter of the water-vapor molecules when the elevon is in the stowed position. Data from the QCM located 20° off the centerline of the nozzle was limited since the sensor became inoperative near the beginning of the experiment.

The effect of temperature of the elevon/fuselage assembly on mass-flux distribution was striking. Shown in graphical form in Figure 10, the "warm case" data indicates a narrowing of the molecular distribution from the nozzle. Although these data do not correlate well with the predicted values, they do suggest a more efficient dismissal of effluent from the nozzle, i.e., more molecules are directed away from the spacecraft. It is then apparent that the cold case data or the molecular distribution predicted by theory probably represent worst-case conditions of distribution of water-vapor molecules from the FES. The reasons for the differences in distributions directly attributable to spacecraft surface temperatures are unclear.

Each data point consisted of a set of 10-20 individual measurements utilizing nuclear instrumentation pulse-counting techniques. Each individual measurement represented an integration (pulse counting) time of 10 seconds. This approach permitted a precision or self-consistency of better than $\pm 2\%$ between measurements. Measurements were reproducible after major configuration changes, e.g., elevon movement, elevon/fuselage temperature changes, and FES flow rate, to better than $\pm 10\%$ for most measurements.

CONCLUSIONS

The directional characteristics of a specially designed, sonic nozzle for the dismissal of water-vapor effluents from the Shuttle Orbiter Flash Evaporator System have been measured for two specific cases. The specific cases include: (1) elevon position (simulated elevon) and (2) elevon/fuselage assembly surface temperature extremes, viz., -100°C and 40°C .

Cryogenically-cooled quartz crystal microbalances have been shown to be remarkably good sensors for measurement of water-vapor plume profiles in vacuo.

The theoretical source-flow technique for modeling the spacecraft contamination in an on-orbit environment and the corollary analytical function for molecular flow from a sonic nozzle are shown to agree closely with the cold-case data measured during this experiment.

Data from the warm ($+40^{\circ}\text{C}$) elevon/fuselage simulator do not correlate well with predicted values. The reasons for poor correlation are not clear. The measured values from the warm case do suggest that the nozzle/surfaces combination is more efficient at directing the water molecules away from the spacecraft. It follows, then, that the cold case data or the molecular distributions predicted by theory probably represent worst-case distributions of water-vapor molecules from the flash evaporator system.

REFERENCES

1. Muscari, J. A. and Westcott, P., "Optical Contamination Evidence from Skylab and Gemini Flights," *Applied Optics*, Vol. 14, No. 12 (1975).
2. Rantanen, R. O. and Ress, E. B., "Payload/Orbiter Contamination Control Assessment Support, Final Report," Martin Marietta Aerospace, June 1975.
3. Jaax, J. R., "Flash Evaporator Subsystem Hardware, Operational and Performance Description," October 1976.
4. Rantanen, R. O. and Jensen, Strange D. A., "Orbiter/Payload Contamination Control Assessment Support, Final Report," Martin Marietta Aerospace, April 1977.
5. Visentine, J. T. and Richmond, R. G. and Kelso, R. M., "Molecular Outgassing Measurements for an Element of the Shuttle Thermal-Protection System," *Thermophysics of Spacecraft and Outer Planet Entry Probes*, AIAA Vol. 56 (1977).
6. Richmond, R. G. and Kelso, R. M., "Effectiveness of the Shuttle Orbiter Payload Bay liner as a Barrier to Molecular Contamination from Hydraulic Fluids," Proceedings International Spacecraft Contamination Conference, Colorado Springs, CO, March 1978.
7. Visentine, J. T., Ehlers, H. K. F., and Roberts, B. B., "Determination of High-Velocity Water-Vapor Plume Profiles in a Thermal-Vacuum Environment," NASA SP-336, November 1975, page 727.
8. Santeler, D. J., Jones, D. W., Holkeboer, D. H., and Pagano, F., Vacuum Technology and Space Simulation, NASA SP-105, page 3.

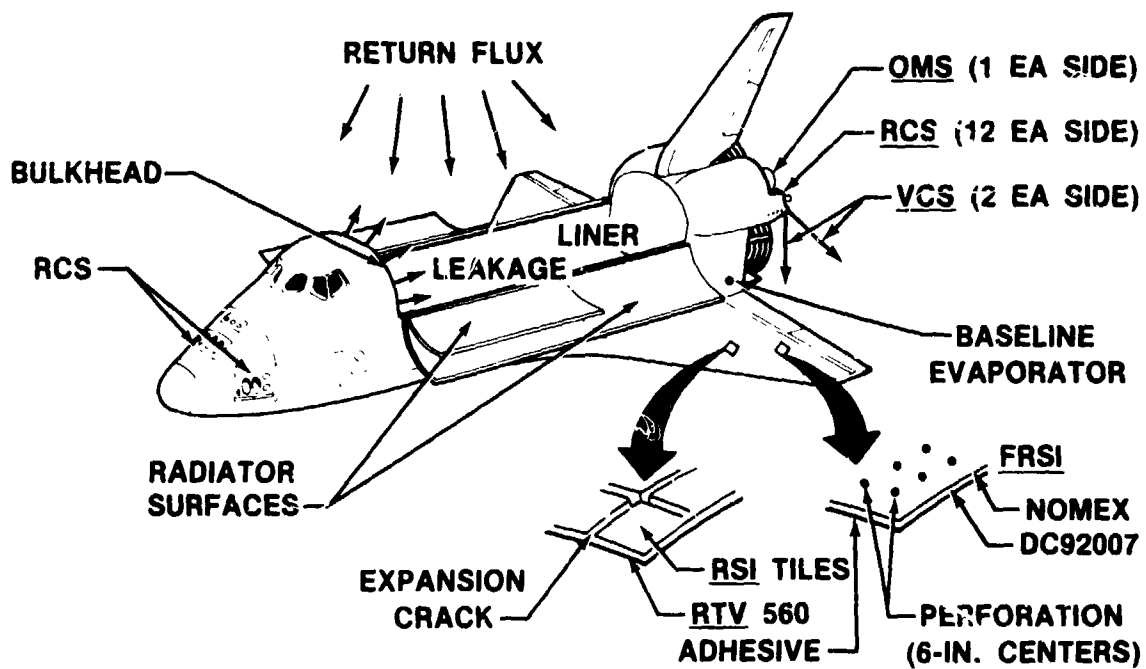


Figure 1.- Major shuttle orbiter source locations.

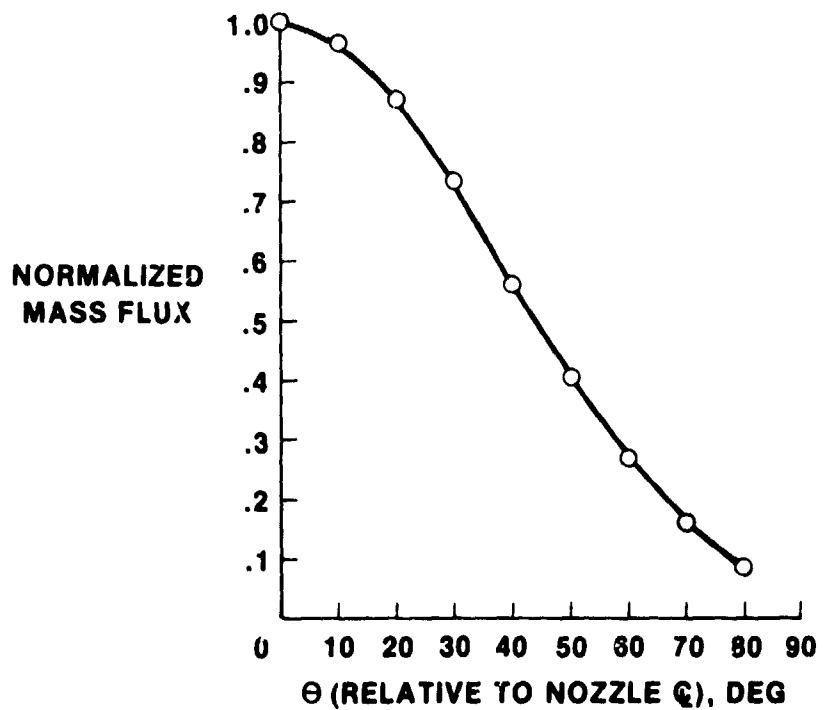


Figure 2.- Predicted normalized mass-flux distribution after ref. 4.



Figure 3.- Flash evaporator test setup in chamber A.

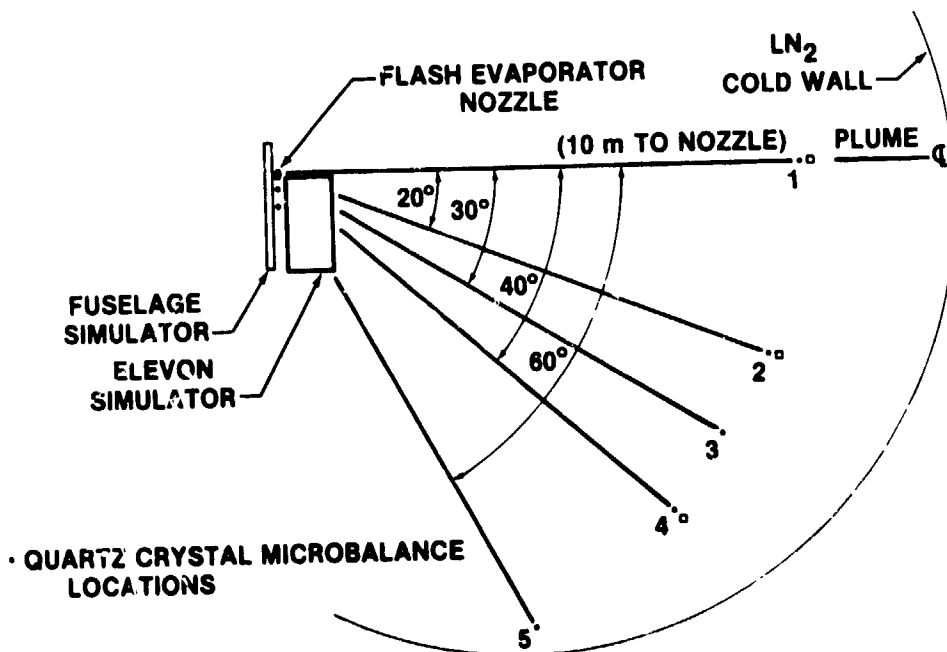


Figure 4.- Chamber A FES primary instrumentation.



Figure 5.- Orbiter fuselage simulator, nozzle, and elevon simulator.

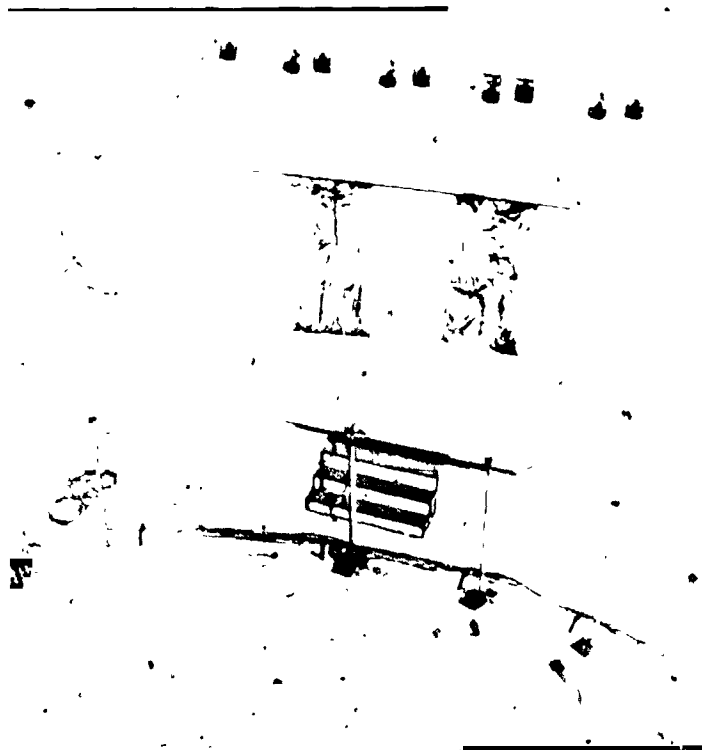


Figure 6.- Plume measurement locations.



Figure 7.- Cryogenically-cooled quartz crystal microbalance and tubulated ionization gage.

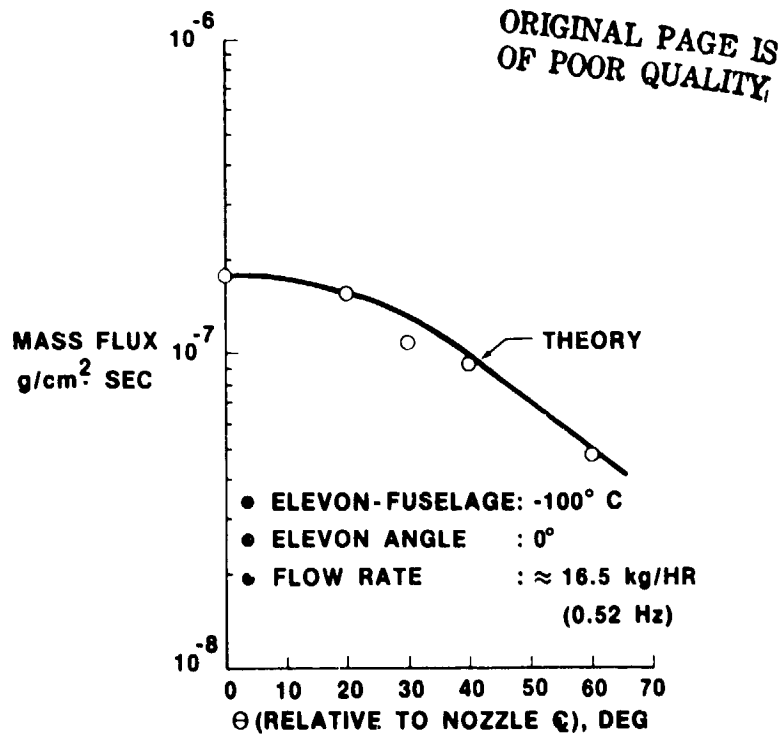


Figure 8.- Typical mass-flux distribution.

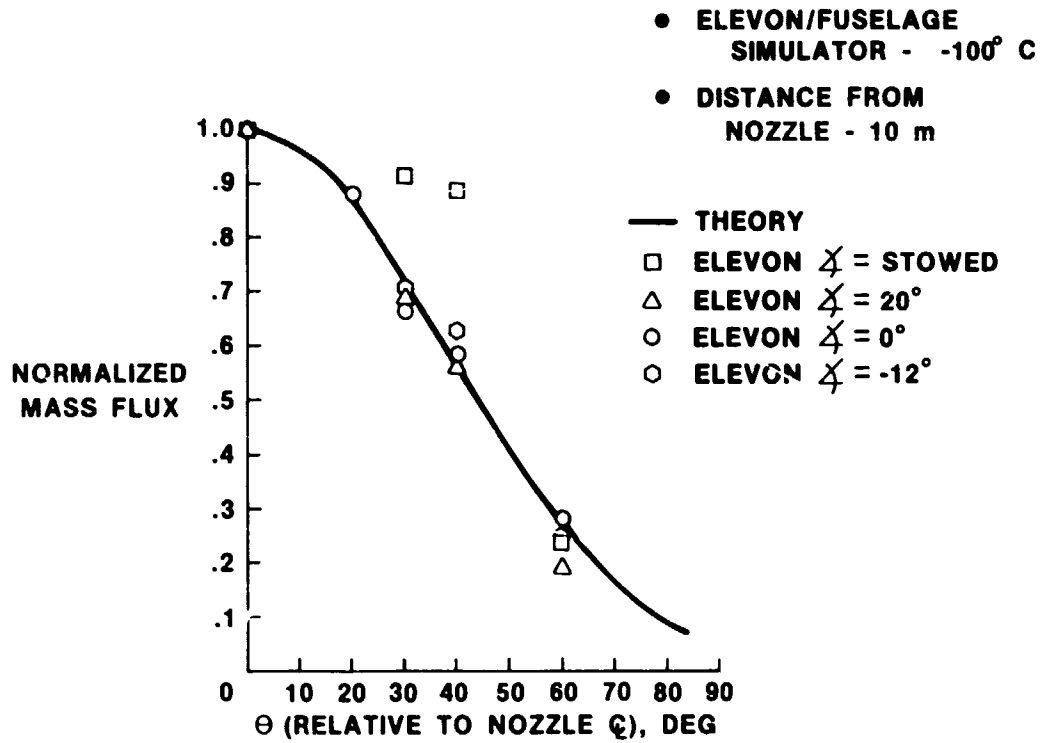


Figure 9.- Effect of elevon angle on mass-flux distribution.

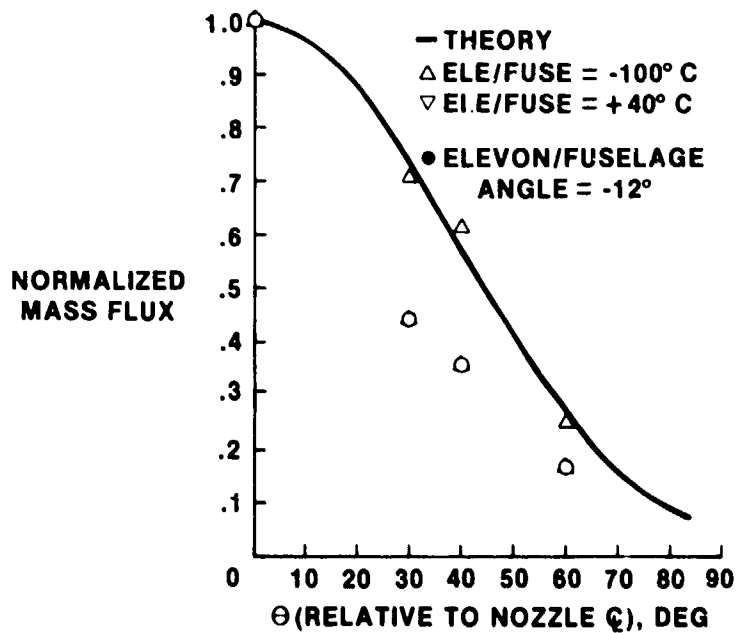


Figure 10.- Effect of elevon/fuselage temperature on mass-flux distribution.